

# COLOR CONSTANCY BEYOND STANDARD ILLUMINANTS

Oguzhan Ulucan, Diclehan Ulucan, Marc Ebner

Institut für Mathematik und Informatik, Universität Greifswald, Greifswald, Germany

## ABSTRACT

The effects of strong color casts in traditional, learning-based and data-driven color constancy algorithms is analyzed. This is the first study investigating the response of color constancy methods to illuminants on the edges and outside the color temperature curve. According to the comprehensive experiments, while traditional studies do not fail to "discount the illuminant" from inputs which have strong color casts, the efficiency of learning-based and data-driven algorithms in obtaining canonical outputs decreases significantly compared to traditional methods. We discuss the reasons behind this performance decay and introduce a traditional color constancy algorithm, which presents competitive results in a challenging dataset.

**Index Terms**— Color Constancy, Illumination Estimation, White Balance

## 1. INTRODUCTION

Colors are not a physical property of objects, but they are the product of the brain [1]. The details of the processing occurring in the brain is still a puzzle awaiting to be solved [2]. Yet, it is known that the human visual system and several other biological vision mechanisms are able to identify the colors in a scene regardless of the illumination conditions [2]. This phenomenon is called *color constancy* and has a significant role in distinct higher level computer vision tasks such as object recognition and image segmentation which are utilized in diverse applications, i.e. robotics and security systems [3].

An image  $I$  with RGB pixel values at position  $(x, y)$  can be represented as [4];

$$I(x, y) = \int_w R(x, y, \lambda)E(x, y, \lambda)S(\lambda)d\lambda, \quad (1)$$

where,  $R(x, y, \lambda)$  is the amount of reflected light,  $E(x, y, \lambda)$  represents the light source,  $S(\lambda)$  is the sensor response characteristics of the capturing device, and  $\lambda$  is the wavelength of the visible spectrum  $w$ . The aim of color constancy is to estimate the color vector of the light source  $\mathbf{L}$ ,

$$\mathbf{L} = [l_R \ l_G \ l_B]^T = \int_w E(x, y, \lambda)S(\lambda)d\lambda. \quad (2)$$

This is an ill-posed problem since both  $E(x, y, \lambda)$  and  $S(\lambda)$  are unknown. For more than four decades, *statistical*-, *gamut*-, *learning-based* and *data-driven* methods have been proposed to provide a solution to the challenging nature of color constancy. While traditional approaches make assumptions relying on the statistical properties and color information of images, learning-based algorithms usually require parameters such as  $S(\lambda)$  and depend on the dataset.

Color constancy datasets and learning-based methods frequently do not include illuminants with values outside the color temperature curve. Although, these lights are ignored, they can be observed in

several applications. For instance, greenish and purplish lights with values outside or on the edge of the color temperature curve can be found in indoor environments due to aesthetic purposes and chromotherapy to treat physical and emotional disorders [5, 6]. Moreover, strong greenish and purplish lights are commonly used in agriculture, i.e. in greenhouses and growth lamps [7]. For example, artificial green lights are sometimes placed into greenhouses, since the stimulation of photosynthesis deep within the leaf is enabled by the absorption of green light, which also contributes to carbon gain [7]. Also, since green light does not disturb the night period of plants it is used to navigate the grow room and inspect plants during their dark cycle. Additionally, it is observed that purple light reduces yellowing and retains chlorophyll in broccoli allowing it to be kept in storage freshly for a longer time [8]. Furthermore, in recent applications green lights are even used for vertical gardening in space stations and spacecrafts [9]. Undoubtedly, in all of the mentioned agricultural applications it is important to ensure a healthy growing and storage environment via detecting diseases, spoilage and insect formation on plants in early stages. However, under out of ordinary lights and especially with unknown camera specifics, computer vision systems using learning-based or data-driven color constancy algorithms as a pre-processing step may have problems in identifying the details of a scene.

In this paper, it is argued that even though they outperform statistical- and gamut-based algorithms on widely used benchmarks, color constancy methods based on neural networks and data-driven approaches have in fact a critical drawback when compared to traditional algorithms. They cannot correct images with illumination values outside the color temperature curve and also illuminants on the edge of the color temperature curve are usually estimated inaccurately. Therefore, data-driven and neural networks-based methods can easily become inefficient in real-life applications. To the best of our knowledge, this is the first study pointing out this problem and conducting comprehensive experiments, which demonstrate that traditional color constancy algorithms produce robust results independent of the input image's properties, while neural networks and data-driven methods' efficiency varies according to the input even though it is usually claimed otherwise. Furthermore, a simple yet effective traditional color constancy algorithm is introduced, which presents state-of-the-art performance in quantitative analyses and is highly competitive in terms of computational complexity.

This paper is organized as follows. Section 2 gives a summary of the state-of-the-art color constancy algorithms. Section 3 introduces the proposed method. Section 4 presents the experiments carried out in the study and discusses the outcomes. Section 5 provides a brief conclusion.

## 2. RELATED WORK

Due to its under-constraint nature, presenting a robust solution to color constancy has been troublesome and many attempts have been made to design a reliable algorithm. In the following, several existing methods, which are also employed during the experiments in Section 4 are explained briefly.

The most well-known color constancy algorithms are max-RGB [10] and gray world [11]. While the max-RGB method is based on the Retinex algorithm and identifies the maximum values of each image channel separately to use them as an estimate of the illuminant to find the color constant descriptor of a scene, the gray world algorithm estimates the illumination of a scene by assuming that the average reflectance of the scene is achromatic. The shades of gray algorithm [12] assumes that the mean of pixels raised to a certain power is gray. The gray-edge hypothesis [13] relies on the assumption that the mean edge difference in an image is achromatic. In the weighted gray-edge algorithm [14], edges providing useful information for illuminant estimation are pointed out during illumination computations. The mean-shifted gray pixel method [15] is a camera-agnostic color constancy method that transforms the task of illumination estimation into gray pixel detection. The adaptive method estimates the scene’s illumination via a novel grayness measure and mean-shift clustering based on the statistical properties of the color-biased image’s gray pixels. The principal component analysis (PCA) based color constancy algorithm [16] estimates the illuminant of the scene by only taking into account the pixels which are informative for describing the illuminant of the scene rather than using all spatial information of the image. The pixels having the largest gradient in the data matrix are selected and given to the PCA algorithm to estimate the illumination of the scene. The physiologically inspired color constancy method [17] is designed from the outcomes of physiological findings on color information processing of the human visual system. The algorithm estimates the illuminant of the scene by taking advantage from the responses of the double opponent cells in LMS space, where L, M and S represent the response of the cone types of the human eye. The idea behind the method originates from the observation that color distributions of the double opponent cells correspond to the color of the light source.

The k-nearest neighbor-based white balance method [18] is a data-driven approach depending on a dataset of 65,000 image pairs and PCA features. It takes an input and searches for the most similar incorrectly white-balanced images in the dataset to compute a color mapping function. The autoencoder-based color constancy approach [19] learns common representations of images and fine-tunes the model to estimate the illumination. By using unlabeled data and reconstructing images via a convolutional autoencoder the algorithm aims to be camera- and scene-independent. The deep white-balance editing method [20] consists of an encoder and decoders, which aim to output images with correct auto, indoor and outdoor white-balance settings. The model is a deep neural network and it is trained in an end-to-end manner. The auto white-balance algorithm [21] does not require an illuminant estimation process to correct the illumination in images. Instead, it renders the input image with certain white-balance settings multiple times and extracts weight maps via a deep neural network to form the final image. In the cross-camera convolutional color constancy method [22], which is an extension of the convolutional color constancy algorithm [23], a camera-independent system is designed to estimate the illuminant of a scene. During the testing phase, apart from the input image, the model also takes in a small set of unlabeled, not auto-balanced arbitrary images to calibrate itself according to the camera’s spectral properties.

## 3. PROPOSED METHOD

As presented in Sec. 2 color constancy studies rely on different approaches. While investigating these methods it is observed that color constancy algorithms, which are inspired from the human visual system, i.e. Retinex algorithm, perform well in estimating the illuminant of a scene regardless of the light source type. The proposed method is inspired from this observation and the indications that the human visual system might be estimating the illuminant of a scene based on both the space-average color of the scene and the highest luminance patch [8]. Thus, to design a simple yet effective and low-cost color constancy algorithm that has a correspondence in the human visual system two assumptions are made: (i) there are several bright pixels somewhere in the scene and (ii) on average, the world is gray. While the effectiveness of the gray world assumption is well-known in the field of color constancy, the advantage of using the brightest pixels of a scene instead of the entire image is discussed in detail in several studies [2, 16, 24, 25].

The proposed algorithm can take both linear-raw data and sRGB images as input. In case it is applied to an sRGB image, the algorithm firstly obtains a linearized image  $\tilde{I}$  in order to remove the gamma correction i.e., to obtain a linear relationship between pixels. Then, linear RGB values are converted into the range [0, 1]. Afterwards, 2% percent of the darkest and the brightest pixels are clipped in order to reduce possible noise. Subsequently, the input image is separated into non-overlapping patches  $\{\tilde{I}_p\}_{p=1}^n$ , where  $\tilde{I}_p$  represents the patch and  $n$  the number of distinct patches, respectively. These blocks cannot be arbitrarily small, because the chance of obtaining uniform-colored patches increases as the size of the patches is reduced. However, the gray world assumption is only valid when an adequate number of distinct colors is present in the scene [26]. It is important to note here that,  $n$  is the only fixed parameter of the proposed algorithm. It is experimentally determined that separating an image into 6 or 8 patches is sufficient to obtain the best results in images with different resolutions while avoiding high computational cost.

Since the algorithm relies on the assumption of max-RGB, in each distinct  $\tilde{I}_p$  it is assumed that for every channel there exists at least one bright pixel which is the most informative element to estimate the illuminant of  $\tilde{I}_p$ . These maximum  $R, G, B$  values can be simply determined via taking the maximum intensity values of each channel in  $\tilde{I}_p$ . Then, these maximum intensity values form the informative intensity vector  $\tilde{I}_{p,max}$ , which can be represented as  $\tilde{I}_{p,max} = [R_{p,max}, G_{p,max}, B_{p,max}]$ . Subsequently, the estimation of the illuminant for each  $\tilde{I}_p$  is carried out via determining how much  $\tilde{I}_{p,max}$  deviates from the gray world. Here it should be noted that if a scene is gray on average, then the summation of the intensity values of  $\tilde{I}_{p,max}$  is assumed to be gray. However, if there is a color cast in the scene, it causes a shift away from the gray world. For every  $\tilde{I}_{p,max}$ , this deviation can be computed by using a scaling vector  $\mathbf{C}_p = [c_r, c_g, c_b]$ , which scales the intensities such that they sum to a gray value. This gray value can be extracted from the input image by simply taking the mean of all pixels, however it is observed that using a single fixed gray value for all  $\tilde{I}_p$  decreases the performance of the proposed method. The reason behind this can be explained with the fact that the surface orientations are not uniform throughout the image, but they differ in local regions. In other words, for every  $\tilde{I}_p$  a different gray value exists, since the surface orientations in each  $\tilde{I}_p$  vary. Thereupon, for each  $\tilde{I}_p$  the gray value is determined by taking the mean of pixels, which fall within the patch of interest.

Consequently, the problem can be simply represented as,

$$c_r \cdot R_{p,max} + c_g \cdot G_{p,max} + c_b \cdot B_{p,max} = \bar{I}_{p,gray} \quad (3)$$

where,  $\bar{I}_{p,gray}$  is the mean of over all channel values of  $\bar{I}_p$ .

Eqn.3 can be easily converted into a constrained optimization problem as follows,

$$\mathbf{C}_p = \arg \min_{\mathbf{C}_p} \left\| \bar{I}_{p,max} \mathbf{C}_p - \bar{I}_{p,gray} \right\|_2 \quad s.t. \quad \forall c \in \mathbf{C}_p \geq 0. \quad (4)$$

Eqn.4 is computed for each  $\bar{I}_p$ . Since it is assumed that there is a global illuminant in the scene, the estimate of the illuminant  $\tilde{\mathbf{L}}$  is calculated by,

$$\tilde{\mathbf{L}} = \sum_{p=1}^n \frac{\mathbf{C}_p}{n}. \quad (5)$$

Lastly, the canonical image is obtained via scaling  $\bar{I}$  according to  $\tilde{\mathbf{L}}$ .

#### 4. EXPERIMENTS AND DISCUSSIONS

As aforementioned, in this paper it is argued that the learning-based and data-driven methods have a critical drawback compared to traditional ones. They do not properly estimate the illuminant of a scene in case the light is outside or on the edge of the color temperature curve. This shortcoming arises from the fact that during algorithm design different illuminant types are neglected. Learning-based and data-driven color constancy algorithms estimate the illumination of a scene based on the training samples, thus naturally they expect the illuminants of scenes in the training and testing sets to be somehow similar [27]. However, in real-world applications where these algorithms are expected to remove color casts as a pre-processing step in a computer vision pipeline, they are likely to face images with different statistical distributions than their training set. Consequently, the performance of learning-based and data-driven methods tends to decrease.

Moreover, input images given to a color constancy algorithm can be captured by a mobile phone or by a camera whose spectral sensitivity is unknown. In this case, learning-based and data-driven algorithms will face an inevitable challenge since commonly employed color constancy datasets are mostly formed by using one camera with fixed spectral sensitivity [27]. As a result, even though learning-based algorithms outperform statistical-based methods on such benchmarks, they have trouble in correcting images with different statistical distributions. This is not a challenge for statistical-based approaches [15]. Based on these observations, in this section comprehensive comparisons are provided to present the performance difference of the traditional and learning-based/data-driven studies. Moreover, the effectiveness of the proposed traditional color constancy algorithm is discussed.

In this study, the experiments are conducted on the modified version of the datasets created in the work of Afifi *et al.* [18]. Only the ground truth images from *The Rendered WB dataset (Set 1 & 2)* are taken and they are assumed to be canonical. Although, Set 1 contains sufficient images for extensive comparisons, Set 2 is also considered since it includes diverse images captured via distinct mobile phones. Several repeating, blurry and defocused images are removed from the dataset. Subsequently, a total of 1504 ground truth images are obtained to create the rendered images under different illuminants both on and outside the color temperature curve. The corresponding RGB values of 2000K, 3500K, 4800K, 5200K and 10000K

are selected for rendering the images with illuminants on the color temperature curve. 4800K, 5200K and 10000K are chosen since they are commonly observed in many datasets. On the other hand, 2000K and 3500K are preferred because they lie close to the edge of the curve which makes them a challenge to several color constancy algorithms. Furthermore, to obtain images with illuminants outside the color temperature curve, strong greenish and purplish colors are selected.

Two different sets of inputs are generated by taking the product of the images and corresponding RGB values of distinct illuminants. Let us assume that  $L_{CTC_i}$  is an array of five vectors, which correspond to the RGB values of a specific illuminant on the color temperature curve, where  $i \in \{2000K, 3500K, 4800K, 5200K, 10000K\}$ . Then, the rendered image  $\hat{I}(x, y)$  can be obtained as follows,

$$\hat{I}(x, y)_i = I(x, y) \cdot L_{CTC_i}. \quad (6)$$

Similarly, the images with illuminants outside the color temperature curve are formed by multiplying  $I(x, y)$  with the corresponding  $\mathbf{L}$ . Subsequently, a total of 7520 images with illuminants on the color temperature curve and 3008 images outside the color temperature curve are created. Example ground truth and rendered images are demonstrated in Fig. 4.

In this study, the proposed method and the algorithms briefly explained in Section 2 are investigated to analyze their performance difference on images with illuminants outside and on the color temperature curve. The experiments are conducted on an Intel i7 CPU @ 2.7 GHz Quad-Core 16 GB RAM machine. All the codes are obtained either from the author's official web-page or via contacting the authors. For each algorithm, the default settings are adopted for comparison without any optimization and the input specifications are met. Also, it is important to note here that the proposed algorithm has not been optimized yet.

Overall, the traditional algorithms Gray-World [11], max-RGB [10], Shades-of-Gray [12], Gray-Edge [13], Weighted Gray-Edge [14], MSGP [15], DOCC [17], PCA-CC [16] and the proposed method are compared against the learning-based methods; DeepWB [20], AWB-MIS [21], C5 [22], C3A [19] and the data-driven technique; WB-sRGB [18]. In order to evaluate the performance of each method, the mean, the median, the mean of the best 25% and the mean of the worst 25% of the angular error, and  $\Delta E$  2000 [28] are reported in Table 3. As presented in Table 3, for both the lights on and outside the color temperature curve, the best mean angular error, median angular error and  $\Delta E$  are achieved by the proposed method with a competitive execution time. Furthermore, especially for images rendered under lights outside the color temperature curve, statistical scores significantly superior to the neural networks based and data-driven approaches are obtained by the proposed algorithm. In Fig. 2, the results for the Gray World, C3A and the proposed method are given for images rendered with diverse illuminants. It is seen that the proposed algorithm is able to successfully estimate the light vector for various types of scenes, which is an observation supported by the low angular errors in Table 3.

Furthermore, in the color constancy studies it is important to reduce not only the mean but also the worst 25% angular error. Hence, obtaining results where the worst cases do not deviate significantly from the mean angular error is desired. As seen in Table 3, the lowest mean of the worst 25% angular error is achieved by the proposed algorithm.

While all traditional algorithms outperformed the neural networks based and data-driven methods in images with illuminants on and outside the color temperature curve, the performance gap between the approaches increased when lights outside the color



**Fig. 1:** Example from the dataset. (Left-to-right) Ground truth and rendered images under 2000K, 3500K, 4800K, 5200K, 10000K, greenish and purplish global illuminant. The color checker is masked out from the images.

**Table 1:** Statistical analysis of the algorithms. The maximum angular error among the color channels is reported. For each metric the best result is highlighted. Average run time of the methods in seconds is reported in the last column.

Algorithms	Lights on the CTC					Lights outside the CTC					Avg. run time
	$\Delta E$	Mean	Median	Best-25%	Worst-25%	$\Delta E$	Mean	Median	Best-25%	Worst-25%	
Gray World	9.239	3.555	1.809	0.670	9.633	10.051	4.305	3.072	1.494	9.139	0.062
max-RGB	7.646	3.657	1.966	0.718	9.536	8.383	4.324	3.117	1.530	9.081	0.043
Shades-of-Gray	7.966	3.626	1.904	0.702	9.688	8.765	4.305	3.086	1.503	9.136	0.125
1 <sup>st</sup> order Gray Edge	7.779	3.659	1.951	0.709	9.740	8.570	4.318	3.089	1.509	9.146	0.184
2 <sup>nd</sup> order Gray Edge	7.765	3.664	1.966	0.709	9.749	8.552	4.316	3.103	1.510	9.139	0.198
Weighted Gray Edge	7.771	3.680	1.983	0.714	9.779	8.477	4.314	3.092	1.511	9.135	0.955
MSGP	3.889	3.436	1.679	0.618	9.483	5.042	4.342	3.151	1.518	9.132	0.290
DOCC	9.127	3.754	2.040	0.732	9.900	13.331	4.401	3.091	<b>1.446</b>	9.515	0.180
PCA-CC	3.659	3.504	1.495	<b>0.554</b>	10.127	4.585	4.345	3.091	1.481	9.270	0.087
<b>Proposed</b>	<b>2.636</b>	<b>3.214</b>	<b>1.427</b>	0.563	<b>9.127</b>	<b>3.768</b>	<b>4.221</b>	<b>3.008</b>	1.462	<b>8.993</b>	0.097
Deep-WB	10.845	7.803	5.315	2.388	17.241	18.337	14.485	13.603	8.006	22.500	0.985
AWB-MIS	11.720	8.393	5.168	1.970	20.313	21.771	15.809	14.586	7.714	26.183	0.826
C5	11.793	9.620	7.115	3.225	20.213	22.196	13.632	13.246	8.956	18.980	0.086
C3A	14.472	4.359	2.296	0.926	11.497	25.860	15.588	13.563	4.065	31.013	<b>0.037</b>
WB-sRGB	11.734	4.933	2.644	1.176	12.395	19.606	25.362	19.694	6.360	52.935	0.334

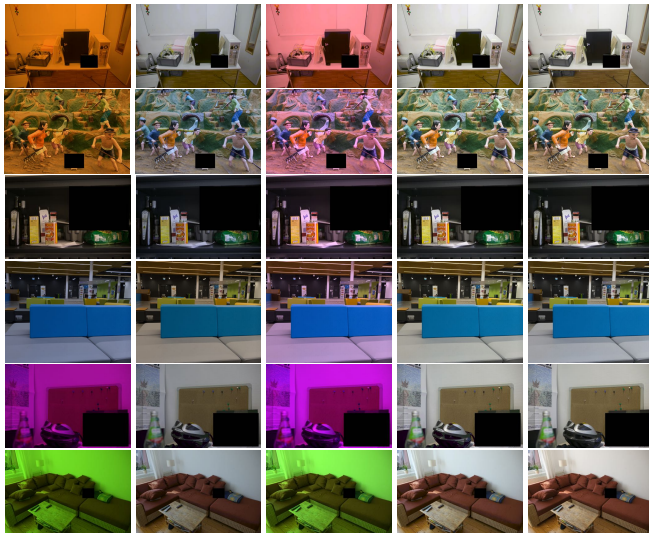


**Fig. 2:** Comparison of algorithms. (Left-to-right) Input image (top-to-bottom: 2000K, 3500K, 4800K, 10000K, purplish and greenish), the result of Gray World, C3A, proposed, and the ground truth image.

temperature curve are present in the image. Even the mean of the best 25% of the angular error of the neural networks based methods resulted in a considerably higher outcome than the traditional approaches. As aforementioned, one reason behind this performance decay is that illuminants outside the color temperature curve are seldomly used for training. Another reason is to perform experiments on datasets with similar statistical distributions. Usually, training and testing operations are carried out on well-known color constancy

benchmarks, which also tend to ignore these lights. Hence, unless a specific adjustment is made to the neural network, the accurate estimation of these illuminants is quite impossible.

It is also noted that although illuminants with corresponding color temperatures of 2000K and 3500K lie on the color temperature curve, neural networks and data-driven methods have difficulty correcting them. The challenge these approaches face is also reflected in their statistical scores as given in Table I. Thus, it can be deduced that the illuminants located on the edge of the color temperature curve are not considered during neural network and dataset creation.

## 5. CONCLUSION

The human visual system easily discounts the illuminant in a scene, while artificial systems have difficulty in carrying out this task. To provide a solution to this challenge, recently, several neural networks based and data-driven color constancy algorithms have been proposed, which outperform traditional methods on well-known benchmarks. In this study, it is demonstrated that the efficiency of these methods decreases when a scene is captured under an illuminant on the edge or outside the color temperature curve, while traditional methods are not affected by the illuminant characteristics of the input image. Furthermore, a simple yet effective traditional color constancy algorithm is designed, which easily discounts out of ordinary illuminants and outperforms existing methods statistically on average with a competitive computational cost.

## 6. ACKNOWLEDGMENTS

The authors are thankful to Firas Laakom for sharing the code of C3A and his delightful discussion.

## 7. REFERENCES

- [1] S. Zeki, *A Vision of the Brain.*, Blackwell Science, 1993.
- [2] M. Ebner, *Color Constancy, 1st ed.*, Wiley Publishing, 2007.
- [3] M. Ebner, "A parallel algorithm for color constancy," *J. Parallel Distrib. Comput.*, vol. 64, pp. 79–88, 2004.
- [4] M. Ebner, "Evolving color constancy," *Pattern Recognit. Lett.*, vol. 27, pp. 1220–1229, 2006.
- [5] R. B. Amber, *Color therapy: Healing with Color*, Aurora Press, 1983.
- [6] E. D. Paragas Jr, A. T. Y. Ng, D. V. L. Reyes, and G. A. B. Reyes, "Effects of chromotherapy on the cognitive ability of older adults: a quasi-experimental study," *Explore*, vol. 15, pp. 191–197, 2019.
- [7] H. L. Smith, L. McAusland, and E. H. Murchie, "Dont ignore the green light: exploring diverse roles in plant processes," *J. Exp. Botany*, vol. 68, pp. 2099–2110, 2017.
- [8] C. Xie, J. Tang, J. Xiao, X. Geng, and L. Guo, "Purple light-emitting diode (LED) lights controls chlorophyll degradation and enhances nutraceutical quality of postharvest broccoli florets," *Scientia Horticulturae*, vol. 294, pp. 110768, 2021.
- [9] E. Darko, P. Heydarizadeh, B. Schoefs, and M. R. Sabzalain, "Photosynthesis under artificial light: the shift in primary and secondary metabolism," *Philos. Trans. Roy. Soc. B: Biol. Sciences*, vol. 369, pp. 20130243, 2014.
- [10] E. H. Land, "The retinex theory of color vision," *Scientific Amer.*, vol. 237, pp. 108–129, 1977.
- [11] G. Buchsbaum, "A spatial processor model for object colour perception," *J. Franklin Inst.*, vol. 310, pp. 1–26, 1980.
- [12] G. D. Finlayson and E. Trezzi, "Shades of gray and colour constancy," in *Color and Imag. Conf.*, 2004, pp. 37–41.
- [13] J. Van De Weijer, T. Gevers, and A. Gijsenij, "Edge-based color constancy," *IEEE Trans. Image Process.*, vol. 16, pp. 2207–2214, 2007.
- [14] A. Gijsenij, T. Gevers, and J. Van De Weijer, "Physics-based edge evaluation for improved color constancy," in *IEEE Conf. Comput. Vision Pattern Recognit.*, 2009, pp. 581–588.
- [15] Y. Qian, S. Pertuz, J. Nikkanen, J.-K. Kämäräinen, and J. Matas, "Revisiting gray pixel for statistical illumination estimation," *arXiv preprint arXiv:1803.08326*, 2018.
- [16] D. Cheng, D. K. Prasad, and M. S. Brown, "Illuminant estimation for color constancy: Why spatial-domain methods work and the role of the color distribution," *J. Opt. Soc. America A*, vol. 31, pp. 1049–1058, 2014.
- [17] S.-B. Gao, K.-F. Yang, C.-Y. Li, and Y.-J. Li, "Color constancy using double-opponency," *IEEE Trans. Pattern Anal. Mach. Intell.*, vol. 37, pp. 1973–1985, 2015.
- [18] M. Afifi, B. Price, S. Cohen, and M. S. Brown, "When color constancy goes wrong: Correcting improperly white-balanced images," in *IEEE Conf. Comput. Vision Pattern Recognit.*, 2019, pp. 1535–1544.
- [19] F. Laakom, J. Raitoharju, A. Iosifidis, J. Nikkanen, and M. Gabbouj, "Color constancy convolutional autoencoder," in *IEEE Symp. Ser. Comput. Intell.*, 2019, pp. 1085–1090.
- [20] M. Afifi and M. S. Brown, "Deep white-balance editing," in *IEEE Conf. Comput. Vision Pattern Recognit.*, 2020, pp. 1397–1406.
- [21] M. Afifi, M. A. Brubaker, and M. S. Brown, "Auto white-balance correction for mixed-illuminant scenes," *arXiv preprint arXiv:2109.08750*, 2021.
- [22] M. Afifi, J. T. Barron, C. LeGendre, Y.-T. Tsai, and F. Bleibel, "Cross-camera convolutional color constancy," in *IEEE Int. Conf. Comput. Vision*, 2021, pp. 1981–1990.
- [23] J. T. Barron, "Convolutional color constancy," in *IEEE Int. Conf. Comput. Vision*, 2015, pp. 379–387.
- [24] H. R. V. Joze, M. S. Drew, G. D. Finlayson, and P. A. T. Rey, "The role of bright pixels in illumination estimation," in *Color Imag. Conf.*, 2012, pp. 41–46.
- [25] E. Lakehal and D. Ziou, "Computer vision color constancy from maximal projections mean assumption," in *Int. Conf. Image Signal Process.*, 2016, pp. 148–156.
- [26] M. Ebner, "Color constancy based on local space average color," *Mach. Vision Appl.*, vol. 20, pp. 283–301, 2009.
- [27] S.-B. Gao, M. Zhang, C.-Y. Li, and Y.-J. Li, "Improving color constancy by discounting the variation of camera spectral sensitivity," *J. Opt. Soc. America A*, vol. 34, pp. 1448–1462, 2017.
- [28] G. Sharma, W. Wu, and E. N. Dalal, "The ciede2000 color-difference formula: Implementation notes, supplementary test data, and mathematical observations," *Color Res. Appl.*, vol. 30, pp. 21–30, 2005.